Spray-Spray and Spray-Wall Interactions in Diesel Sprays from Micro-Hole Nozzles under Ultra-High Injection Pressures

W. Zhang[1*], K. Nishida[1] and J.-P. Tian[2]
[1]Department of Mechanical System Engineering, University of Hiroshima
Higashi-Hiroshima 739-8527, Japan
[2]Institute of Internal Combustion Engine, Dalian University of Technology
Dalian 116023, China

Abstract

In direct injection (D.I.) Diesel engines, injection parameters have a significant influence on the spray evolution, mixture preparation, combustion, and emission formation processes. It has been approved that decreasing nozzle hole diameter and increasing injection pressure are the two effective approaches to improve the spray and combustion characteristics. In the past research, the spray from a micro-hole nozzle (d = 0.08 mm) under an ultra-high injection pressure (P_{inj} = 300 MPa) has been comprehensively studied. To correlate the results of the single-hole nozzle to the multi-hole one and to clarify the effects of spray-spray and spray-wall interactions on the entrainment and vaporization processes, the present work focuses on the mixture formation process of a two-hole nozzle with a hole diameter of 0.08 mm under different wall-impinging conditions. The laser absorption-scattering (LAS) technique was employed to obtain the qualitative and quantitative information under various conditions. The evolution of both the liquid and vapor phases fuel was recorded. An asymmetric image processing method was used to acquire the data on the fuel vaporization and the projected vapor mass distribution. The experiments were carried out in a quiescent constant-volume vessel. The test ambient conditions were the same as those at the start of injection in the real engine. Firstly, the free spray and the flat-wall-impinging spray were investigated. Then, to simulate the engine-like wall-impinging spray process, two kinds of two-dimensional (2-D) piston cavity shape walls, the shallow dish type and the reentrant type, were designed according to the shape of the combustion chamber in the prototype engine. The interactions between the spray and the flat wall, between the spray and the curved wall, and between the sprays were discussed respectively. The results provide useful information for understanding the detailed evolution of Diesel sprays and for implementing the micro-hole nozzle and the ultra-high injection pressure in D.I. Diesel engines.

Introduction

Exhaust emissions from the modern direct injection (D.I.) Diesel engines have been reduced significantly in recent years, but the more stringent emission standards for particulate matters (PM) and nitrogen oxides (NOx) require further improvements on the mixture formation and combustion processes. A great deal of research work has been conducted on improving the in-cylinder process by adjusting the parameters of the injection system. The rapid development in the Diesel engine technology has resulted in a dramatic increase in the injection pressure and in a decrease in the nozzle hole diameter [1]. High pressure fuel injections have been found to be effective for improving the Diesel engine performance and for reducing the PM emission [2-5]. The increased injection pressure is also capable of enhancing the vaporization rate and the mixture preparation, thus resulting in a decrease in the ignition delay [6]. At the same time, in various published experimental results, Diesel engine emissions are reduced greatly by decreasing the nozzle hole diameter [7-10]. The combination of the ultra-high injection pressure and the micro-hole nozzle has been proved to be effective for implementing the premixed compression ignition (PCI) combustion concept in D.I. Diesel engines [11]. However, since there is a large discrepancy between the measured results using the optical diagnostics and the predicated results using current predicative models [12], more experimental investigations are required for a fundamental understanding of the governing mechanisms.

The authors have investigated the free and flat-wall-impinging sprays injected from a micro-hole nozzle (d = 0.08 mm) under an ultra-high injection pressure (P_{inj} = 300 MPa). A comprehensive description of the effects of the increased injection pressure and the reduced nozzle hole diameter on the spray tip penetration, the ambient gas entrainment, and the fuel vaporization has been presented in the previous papers [13, 14]. In small-bore high-speed

*Corresponding author, zhangwu-scl@hiroshima-u.ac.jp

D.I. Diesel engines, information on the spray-spray and spray-wall interactions is critical both for improving the design of the injection system and for developing the predictive models. Therefore, in this research work, the attention was focused on the spray from a two-hole nozzle impinging on the 2-D piston cavity shape walls. The objective is to provide qualitative and quantitative information on the spray evolution and the fuel vaporization under different impingement conditions using the laser absorption-scattering (LAS) technique.

Experimental Apparatus and Conditions

Figure 1 shows the experimental set-up of both the injection and LAS systems. A manually operated piston screw pump, high pressure generator (High Pressure Equipment Co., Model 37-5.75-60), was employed to generate an ultra-high injection pressure up to 300 MPa. A Diesel injector, electronically controlled by an injector driver, was specially designed to meet the requirement for ultra-high injection pressures. The second harmonic (visible light, 532 nm) and the fourth harmonic (ultraviolet (UV) light, 266 nm) of an Nd:YAG laser (Continuum NY61-10) were selected as the incident lights. The two beams were initially coaxial and were separated into a Visible beam and a UV beam by a dichroic mirror. The separated beams were expanded and made coaxial again. Then the beams were directed to a fuel spray. After being attenuated by the spray, the beams were separated and focused to two CCD cameras (Hamamatsu Photonics, C4880). A pulse generator (Stanford Inc., DG535) was used to synchronize the Nd:YAG laser, the CCD cameras, and the injection system. For all of the spray types, the asymmetric image processing method was adopted to acquire the information on the fuel vaporization and the vapor fuel mass distributions per unit projected area. The detailed principles of the LAS system, the image processing method, and the measurement accuracy analysis were described in the previous papers [15-17].

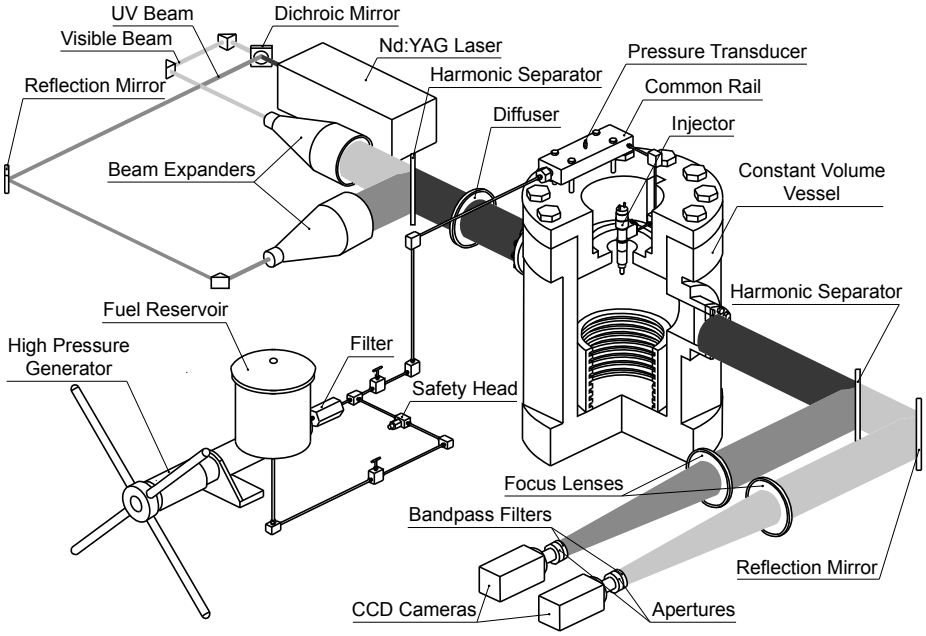

Figure 1. Experimental set-up of injection and LAS systems

Table 1. Experimental conditions

Ambient Gas Density (kg/m^3)	11 (-20 deg.ATDC)			
Ambient Gas Pressure (MPa) /Temperature (K)	2.6/797			
Test Fuel	1,3-Dimethylnaphthalene			
Spray Type	Free	Flat Wall Impinging	2-D Wall Impinging	
Nozzle Hole Diameter (mm)	0.16		0.08	
Nozzle Type	Single-Hole		Single-Hole	Two-Hole
Injection Pressure (MPa)	100		300	
Injection Duration (ms)	2.2		1.3	
Injection Quantity (mg)	15.47		3.87	7.74

The experimental conditions are summarized in **Table 1**. Dimethylnaphthalene (DMN), a test fuel of the LAS technique, was used as the simulator for Diesel fuel. Measurements were made of the three types of sprays including the free, flat-wall-impinging, and 2-D piston cavity shape wall impinging sprays. The conventional nozzle with a hole diameter of 0.16 mm and the objective nozzle with a hole diameter of 0.08 mm were tested. The attention was focused on the micro-hole nozzle under the ultra-high injection pressure. For the micro-hole nozzle, both of the single- and two-hole were investigated. **Figure 2** shows the configuration of the two-hole nozzle. The hole diameter was 0.08 mm. The length of the nozzle hole was 1.2 mm. The included angle between the axes of two cylindrical holes was 23.7 deg, which is the same as that in a multi-hole nozzle. For the free and flat wall impinging sprays the optical path is normal to the cross-sectional plane shown in **Fig. 2**. For the 2-D piston cavity shape wall impinging sprays, to exactly simulate the impingement points of a multi-hole nozzle, the two-hole nozzle was mounted with an offset angle of 51 deg. **Figure 3** schematically shows the shallow dish and reentrant piston cavity shapes and the impingement points at the timing of -20 deg.ATDC. The ambient conditions of the experiments in the constant-volume vessel were the same as those at this timing in the prototype engine. Since in a multi-hole nozzle there were 18 micro-holes that were arranged in a zigzag shape, two spray umbrella angles, 120 and 150 deg, were investigated to clarify the effect of the impingement point.

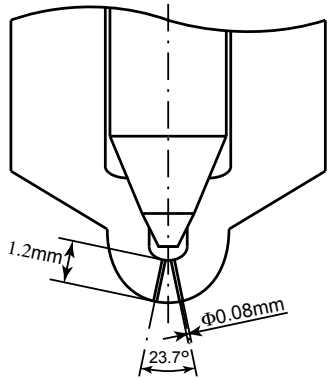

Figure 2. Nozzle tip configuration

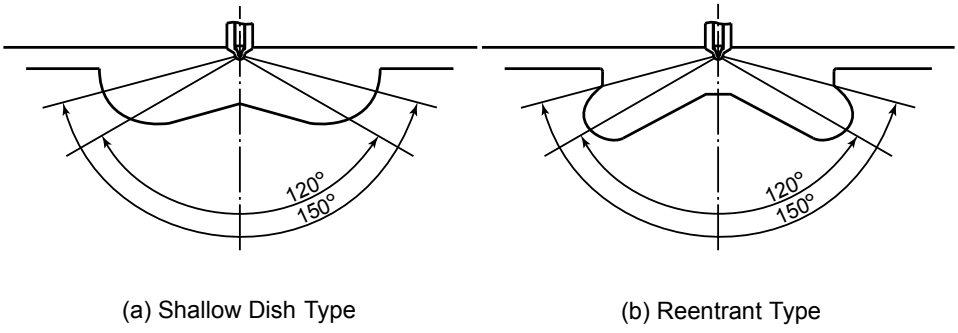

Figure 3. Piston cavity shapes and impingement points at -20 deg.ATDC

Results and Discussion

Effect of Interactions between Spray and Flat Wall

The measured ratio of the fuel vapor mass to the total injected fuel mass at various timings was plotted against the time after the start of injection (SOI) in **Fig. 4**. For the 0.16 mm nozzle, the data close to the end of injection cannot be acquired because the long spray tip penetration exceeds the window range limit of the constant volume vessel. The fuel vaporization was characterized by the ratio of fuel vapor mass to the total injected fuel mass

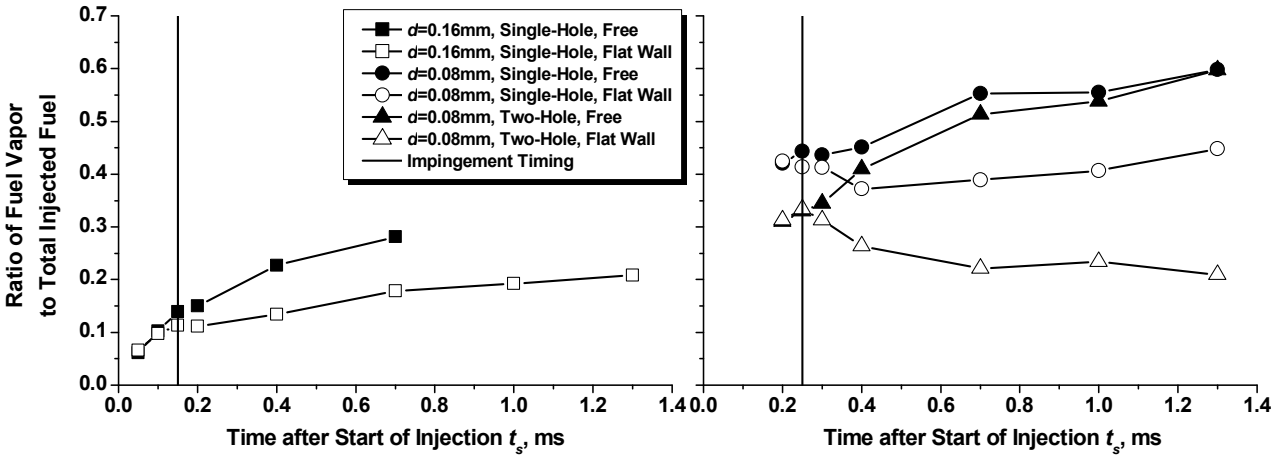

Figure 4. Ratio of fuel vapor to total injected fuel versus time after SOI for free and flat-wall-impinging sprays

(M_v/M_f). Comparison of **Figs. 4(a)** and **4(b)** shows that the fuel vaporization was intensified significantly with increasing the injection pressure and with decreasing the nozzle hole diameter. The 0.08 mm nozzle has a much higher value of M_v/M_f at the initial stage of the injection duration when compared with the 0.16 mm nozzle. The vertical lines in **Fig. 4** stand for the impingement timings under different conditions. It is clearly shown that, for all test cases, M_v/M_f decreases slightly after the wall impingement. After a while, M_v/M_f was reduced by about 35% for the 0.16 mm nozzle, whereas it was only reduced by about 25% for the 0.08 mm nozzle. This might be caused by the less fuel film formed on the wall surface and the stronger secondary breakup after the wall impingement for the spray from the 0.08 mm nozzle under 300 MPa. It is worth noting that M_v/M_f was reduced by more than 50% for two-hole nozzle. The spray-spray interactions after the wall impingement may account for this phenomenon and will be discussed in the later section.

To show the impingement process clearly, the optical thickness images of the liquid and vapor phases acquired by the LAS technique are shown in **Fig. 5**. The right two columns show the flat-wall-impinging sprays at the impingement timings. The left two columns are the free sprays at the corresponding timings. It is obvious that the spray spreading angle is increased for 0.08 mm and 300 MPa. It means more ambient gas is entrained into the spray plume, thus resulting faster atomization and vaporization. After the spray tip impinging on the wall surface, the wall jet penetration is also increased. The ultra-high injection pressure enhances the spray-wall interaction and intensifies the mixing after the impingement. The data on the two-hole nozzle in **Fig. 5(c)** show that there are almost no interactions between the two spray plumes at the free spray region. This is the reason why the fuel vaporization processes shown in **Fig. 4(b)** are similar for two cases of free sprays. The difference between the single- and two-hole nozzles during the initial stage might be caused by the different internal flow and primary breakup mechanism, which will be justified by further experimental and numerical investigations and is out of the scope of this paper.

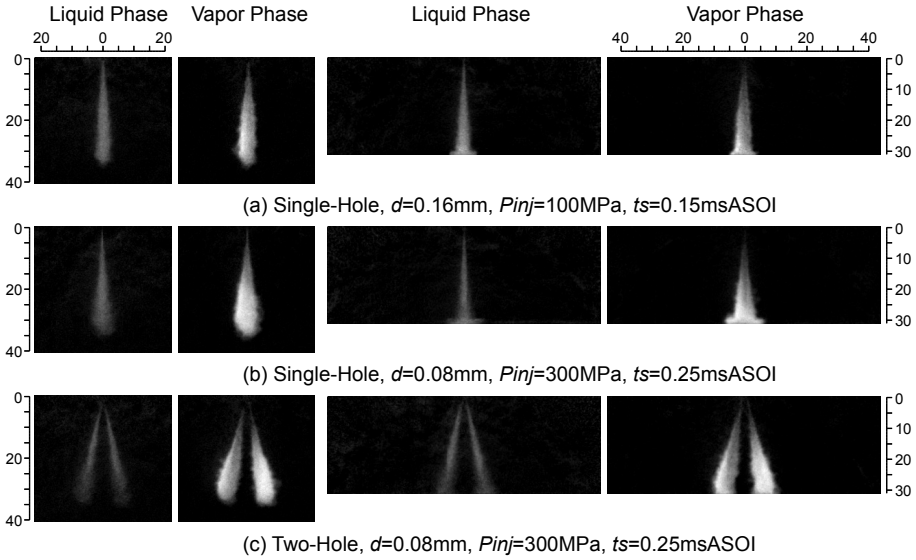

Figure 5. Optical thickness images of liquid and vapor phases at impingement timings

Effect of Interactions between Spray and Curved Wall

Figure 6 shows the measured ratio of the fuel vapor mass to the total injected fuel mass versus the time after SOI for 2-D piston cavity shape wall impinging sprays. Note that the effect of the wall shape on the fuel vaporization is unpronounced for the test conditions with an umbrella angle of 150 deg. For 120 deg, however, the influence becomes significant, which can be explained by examining **Figs. 6** and **7**. When the umbrella angle of 150 deg was adopted, the impingement point was located close to the edge of the piston cavity. After the wall impingement, the major portion of the spray flows out of the cavity for the shallow dish type wall, and it flows to the nozzle tip region for the reentrant type wall. The comparable projected areas at the end of injection shown in **Figs. 7(a)** and **7(b)** indicate the similar development speed for these two conditions, which accounts for the similar fuel vaporization. When the umbrella angle of 120 deg was adopted, the impingement point was translated to the bottom of the cavity where the curvature becomes larger. Therefore, the spray development is confined by the wall and the entrainment process is inhibited significantly. This is the reason why M_v/M_f has the smallest value for 0.08 mm, 120 deg, and reentrant type wall.

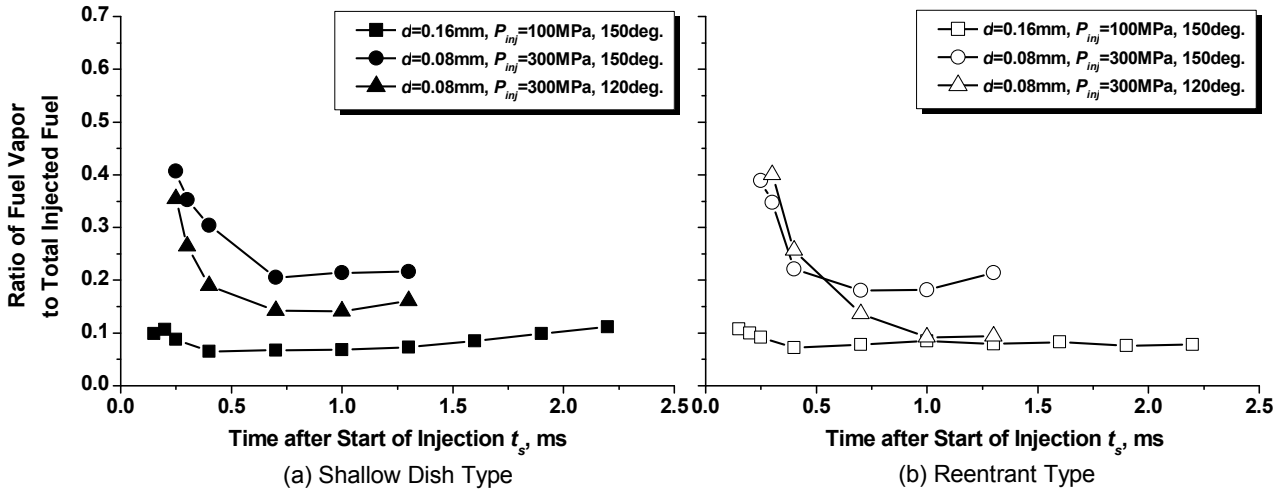

Figure 6. Ratio of fuel vapor to total injected fuel versus time after SOI for 2-D piston cavity shape wall impinging sprays

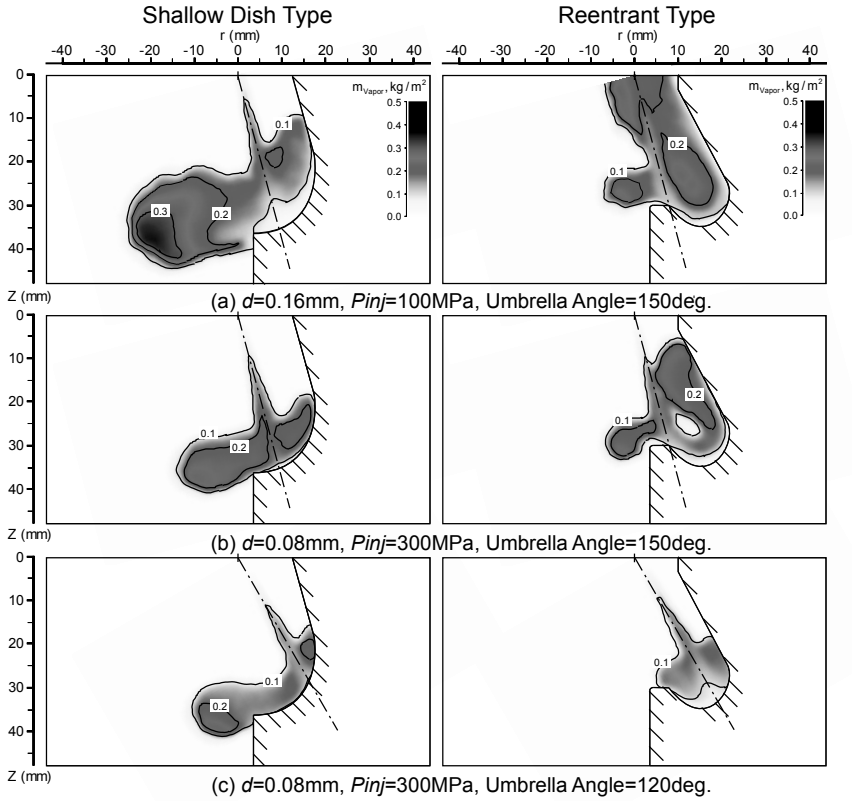

Figure 7. Vapor mass distributions per unit projected area at end of injection

Effect of Spray-Spray Interactions

As discussed above, the weak spray-spray interactions for free sprays result in the similar fuel vaporization process for the single- and two-hole nozzles. For the flat-wall-impinging spray from the two-hole nozzle, the decrease in M_v/M_f is the largest. By examining the spray images, it is found that the two spray plumes interact to each other after the wall impingement. At the end of injection the central region has the highest liquid fuel concentration. It means that, although the initial droplet size is very small for the 0.08 mm nozzle, some droplets interact and coalescent after the wall impingement. Consequently, the fuel vaporization rate decreases. This spray-spray interaction also occurs for 2-D piston cavity shape wall impinging sprays. As shown in **Fig. 8**, although there are obvious difference between the flat-wall-impinging and 2-D wall impinging sprays during the initial stage of the injection dura-

tion, M_v/M_f achieves the similar value at the end of injection. It is of interest to note that this value is between the values for single-hole nozzle sprays with 150 and 120 deg (**Fig. 6**). This indicates that the spray-spray interactions after the wall impingement compromise the difference between 150 and 120 deg.

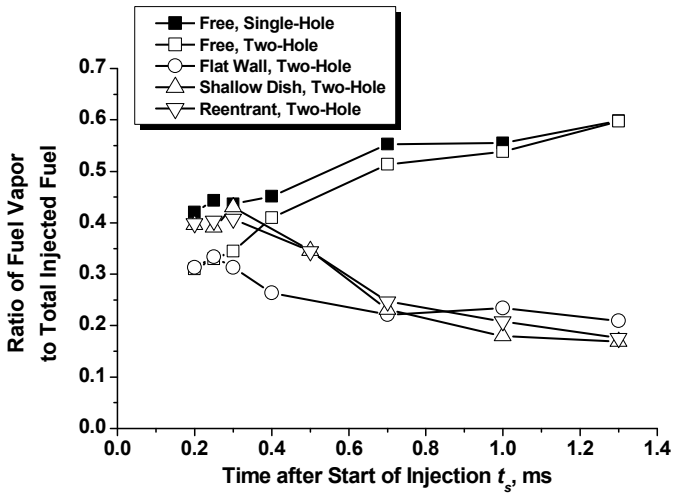

Figure 8. Ratio of fuel vapor to total injected fuel versus time after SOI for sprays from single- and two-hole nozzles

Conclusions

The spray and mixture formation processes of the Diesel sprays from single- and two-hole nozzles were investigated using the LAS technique. The free, flat-wall-impinging, and 2-D piston cavity shape wall impinging sprays were characterized. The spray evolution, the impingement process, and the fuel vaporization were discussed based on the experimental results. Main conclusions are summarized as follows:

1. For the sprays from single-hole nozzles, the effect of the wall impingement on the fuel vaporization decrease as the injection pressure increases and the nozzle hole diameter decreases. For the sprays from a two-hole nozzle, the spray-spray interactions after the wall impingement results in a further decrease in the fuel vaporization. This might be caused by the droplets coalescence during the interaction between two spray plumes.
2. For the sprays from single-hole nozzles impinging on the curved wall surface, the impingement point and the curvature are critical for the fuel vaporization process. The larger curvature at the impingement point causes more fuel flows out of the cavity, thus resulting in stronger gas entrainment and higher fuel vaporization.
3. For the sprays from the two-hole nozzle impinging on the curved wall surface, the spray-spray interactions after the wall impingement compromise the effects of the impingement point and the wall shape on the fuel vaporization.

Acknowledgements

This research work was financially and technically supported by ISUZU Advanced Engineering Center, Ltd.

References

1. G. J. Smallwood, and O. L. Gulder, *Atomization and Sprays* 10:355-386 (2000).
2. T. Kato, K. Tsujimura, M. Shintani, T. Minami, and I. Yamaguchi, *SAE Paper* 890265.
3. D. A. Pierpont, and R. D. Reitz, *SAE Paper* 950604.
4. T. F. Su, and P. V. Farrell, *Atomization and Sprays* 8:83-107 (1998).
5. L. G. Dodge, S. Simescu, G. D. Neely, M. J. Maymar, D. W. Dickey, and C. L. Savonen, *SAE Paper* 2002-01-0494.
6. S. Kobori, T. Kamimoto, and A. A. Aradi, *International Journal of Engine Research* 1:29-39 (2000).
7. D. T. Montgomery, M. Chan, C. T. Chang, P. V. Farrell, and R. D. Reitz, *SAE Paper* 962002.
8. P. Bergstrand, and I. Denbratt, *SAE Paper* 2001-01-2010.
9. J. Benajes, S. Molina, K. De Rudder, D. Maroteaux, and H. B. H. Hamouda, *Proceedings of the Institution of Mechanical Engineers, Part D: Journal of Automobile Engineering* 220:1807-1817 (2006).
10. G. Fenske, J. Woodford, J. Wang, E. El-Hannouny, R. Schaefer, and F. Hamady, *SAE Paper* 2008-01-1595.
11. N. Shimazaki, A. Minato, and T. Nishimura, *International Journal of Engine Research* 8:259-270 (2007).
12. S. C. Kong, Y. Sun, and R. D. Rietz, *Journal of Engineering for Gas Turbines and Power - Transactions of the ASME* 129:245-251 (2007).
13. K. Nishida, W. Zhang, and T. Manabe, *SAE Paper* 2007-01-1890.
14. W. Zhang, K. Nishida, J. Gao, and D. Miura, *Proceedings of the Institution of Mechanical Engineers, Part D: Journal of Automobile Engineering* 222:1731-1741 (2008).
15. Y. Zhang, T. Yoshizaki, and K. Nishida, *Applied Optics* 39:6221-6229 (2000).
16. Y. Zhang, and K. Nishida, *Combustion Science and Technology* 176:1465-1491 (2004).
17. Y. Matsumoto, J. Gao, and K. Nishida, *Transactions of JSAE* 39:177-182 (2008).